Development 122, 3117-3131 (1996)
Printed in Great Britain © The Company of Biologists Limited 1996
DEV4715

Neuronal cell migration in *C. elegans*: regulation of Hox gene expression and cell position

Jeanne Harris[1], Lee Honigberg[1,2], Naomi Robinson[1,2,*] and Cynthia Kenyon[1,2,†]

[1]Department of Biochemistry and Biophysics, and [2]University of California, San Francisco, San Francisco, CA 94143-0554, USA

*Present address: Department of Biology, Texas Wesleyan University, Fort Worth, TX 76105-1536, USA
†Author for correspondence

SUMMARY

In *C. elegans*, the Hox gene *mab-5*, which specifies the fates of cells in the posterior body region, has been shown to direct the migrations of certain cells within its domain of function. *mab-5* expression switches on in the neuroblast QL as it migrates into the posterior body region. *mab-5* activity is then required for the descendants of QL to migrate to posterior rather than anterior positions. What information activates Hox gene expression during this cell migration? How are these cells subsequently guided to their final positions? We address these questions by describing four genes, *egl-20*, *mig-14*, *mig-1* and *lin-17*, that are required to activate expression of *mab-5* during migration of the QL neuroblast. We find that two of these genes, *egl-20* and *mig-14*, also act in a *mab-5*-independent way to determine the final stopping points of the migrating Q descendants. The Q descendants do not migrate toward any obvious physical targets in wild-type or mutant animals. Therefore, these genes appear to be part of a system that positions the migrating Q descendants along the anteroposterior axis.

Key words: cell migration, Hox gene, *mab-5*, *C. elegans*, development

INTRODUCTION

Cell migrations play an important role in development. Concerted movements of large numbers of cells help to establish the different tissue layers during gastrulation and the migrations of individual cells contribute to tissue organization and body pattern. For example, cells of the vertebrate neural crest migrate from their birth place over the neural tube to different locations throughout the body, generating widely distributed neuronal and non-neuronal tissues. Invertebrates such as *Hydra*, *C. elegans* and *Drosophila* all require cell migration to develop normally (Hedgecock et al., 1987; Teragawa and Bode, 1990; Montell, 1994). For cell movement to be a reproducible part of development, the migrations of these cells must be guided. Some cells migrate towards a visible target that supplies a guidance cue; for example, germ cells are attracted to and migrate towards the genital ridge in mammals (Godin et al., 1990). However, many migrating cells stop at positions that are not associated with any obvious physical structures.

A number of genes required for cell migration have been identified in the nematode *C. elegans*. The migrations of the sex myoblasts in hermaphrodites are guided by an attractive signal from the developing gonad mediated by an FGF receptor (Devore et al., 1995). Dorsoventral (D/V) migrations in *C. elegans* are guided by the netrin UNC-6 (Hedgecock et al., 1990; Ishii et al., 1992) in a highly conserved process that has also been shown to guide D/V migrations of axons in the developing vertebrate nervous system (Kennedy et al., 1994; Serafini et al., 1994). The guidance of migrations along the anteroposterior (A/P) axis in *C. elegans* has been shown to involve the gene *vab-8*, which is required for the posterior migration of many cells and axons (Wightman et al., 1996). However, in general, the guidance of cells along the A/P axis is less well understood.

We have chosen to focus on the migrations of the neuroblasts QL and QR, which migrate along the A/P body axis in *C. elegans*. The Q cells are similar to neural crest cells in that they delaminate from an epidermal epithelium and go on to populate regions of the body with sensory neurons (Sulston and Horvitz, 1977; Chalfie and Sulston, 1981). The Q cells and their descendants migrate to highly reproducible positions in a relatively uniform region of the body. QL and QR are born in the same A/P position on opposite sides of the animal: QL on the left and QR on the right. Although they undergo an identical sequence of cell divisions, the two Q cells and their descendants migrate in opposite directions: QL and its descendants migrate towards the posterior, whereas QR and its descendants migrate towards the anterior (Sulston and Horvitz, 1977) (Fig. 1).

The *C. elegans* Hox genes *lin-39* and *mab-5* play important roles in regulating the migrations of cells in the Q lineages. *lin-39*, the *C. elegans Sex combs reduced* homolog that specifies cell fates in the mid-body region, is required for the anterior migration of the QR descendants (Clark et al., 1993; Wang et al., 1993). *mab-5*, the *C. elegans Antennapedia* homolog that specifies cell fates in the posterior body region, is required for the posterior migration of the QL descendants (Chalfie and Sulston, 1981; Kenyon, 1986). Salser and Kenyon (1992) have

shown that *mab-5* acts as a switch to determine the direction of migration. If *mab-5* is ON, the Q descendants migrate towards the posterior; if *mab-5* is OFF, the Q descendants migrate towards the anterior (Salser and Kenyon, 1992; Fig. 1). Here, we extend these results by using a laser microbeam to activate a *heat-shock-mab-5* fusion gene (Salser and Kenyon, 1992) exclusively within a migrating cell. Our findings, together with previous genetic mosaic analysis (Kenyon, 1986), argue that *mab-5* acts within migrating Q descendants to determine their direction of migration.

The state of *mab-5* expression within QL or QR determines whether their descendants will migrate to anterior or posterior positions. However, additional information is required to specify the final positions of these cells, since each QL descendant migrates to a characteristic position in the posterior and each QR descendant migrates to a characteristic position in the anterior. There are no obvious cellular targets located at these stopping points.

To understand better how these cells find their characteristic positions along the A/P axis, we have identified and characterized mutants in which cells in the Q lineage migrate to incorrect positions. Here we show that four of these genes, *egl-20*, *mig-14*, *mig-1* and *lin-17*, are required to activate the Hox gene *mab-5* in the migrating QL cell. When these gene activities are reduced or eliminated, QL and its descendants do not express *mab-5* and consequently QL's descendants migrate towards the anterior. Two of the genes, *egl-20* and *mig-14*, also act in a *mab-5*-independent way to determine the final stopping points of the migrating Q descendants along the A/P axis. Whether or not cells in the Q lineage are provided with *mab-5* activity, in the absence of *egl-20* or *mig-14* gene activities, they migrate to positions shifted posterior to the positions that they would otherwise seek: cells that would migrate posteriorly go too far and cells that would migrate anteriorly stop short. In addition, cells that would remain stationary migrate posteriorly, and cells that would only migrate a short distance anteriorly instead reverse direction and migrate posteriorly. Thus, in addition to activating *mab-5* expression in the migrating QL cell, *egl-20* and *mig-14* appear to participate in a guidance system that determines the final stopping points of cells in the Q lineage.

The gene *lin-17*, which we show activates expression of the Hox gene *mab-5* in the neurobast QL, is homolgous to the *Drosophila* tissue polarity gene *frizzled* (Sawa et al., 1996) and is required for the generation and orientation of cellular asymmetry in many tissues (Sternberg and Horvitz, 1988). Similarly, *egl-20* and *mig-14* also regulate the orientation of certain asymmetric cell divisions (J. H., Jennifer Whangbo and C. K., unpublished data). Thus *egl-20, mig-14, mig-1* and *lin-17* are part of a regulatory system that may be similar to the signaling systems that regulate tissue and segment polarity in *Drosophila*.

MATERIALS AND METHODS

General procedures, nomenclature and strains

Methods for routine culturing and genetic analysis are described in Brenner (1974) and Sulston and Hodgkin (1988). Analyses were performed at 25°C, unless otherwise noted. The wild-type strain N2 is the parent of all strains used with the exception of *egl-20(n1437)*, which was isolated in an MT2878 background (G. Garriga, personal communication). Mutations not described in this paper are described by (Hodgkin et al., 1988) or are noted below.

Mutations used

LG I: *lin-17(n671)*, *lin-17(n677)*, *lin-17(e1456)* (Ferguson and Horvitz, 1985) *mig-1(e1787)*, *mig-1(mu72)*, *mig-1(n687)*, *mig-1(n1354)*, *mig-1(n1652)* (Desai et al., 1988), *lin-6(e1466)*, *dpy-5(e61)*, *jeIn1[mec-7-lacZ+pRF4(rol-6d)]* (Hamelin et al., 1992).
LG II: *mig-14(mu71)*, *mig-14(k124)* (Kiyoji Nishiwaki, personal communication), *rol-1(e91)*, *unc-52(e444)*.
LG III: *mab-5(e1239)*, *mab-5(e2088)*, *mab-5(e1751gf)* (Hedgecock et al., 1987; Salser and Kenyon, 1992), *pag-1(ls2)* (Guofeng Xie and Eric Aamodt, personal communication).
LG IV: *unc-24(e138)*, *dpy-20(e1282)*, *egl-20(n585)*, *egl-20(n1437)*, (Desai et al., 1988) *egl-20(mu25)*, *egl-20(mu27)*, *egl-20(mu39)*, *unc-31(e169)*, *muIs6 [lin-39-lacZ + pRF4(rol-6d)]* (Wang et al., 1993).
LG V: *him-5(e1490)*.
LG X: *mig-13(mu31)* (Robinson, 1995), *muIs5 [lin-39-lacZ + pRF4(rol-6d)]* (Wang et al., 1993), *muIs9[hs-mab-5 + C14G10(unc-31$^+$)]* (Salser et al., 1993).
Rearrangements: *eDf19*, *tDf3*, *tDf4* (Ahn and Fire, 1994), *jDf1*, *jDf2*, *jDf4* (Jacobson et al., 1988).

Isolation of mutants with misplaced QL descendants

mig-14(mu71) and *mig-1(mu72)* were isolated in a screen for mutants with misplaced Q descendants. In order to visualize the Q descendants using a dissecting microscope, we used a *mec-7-lacZ* fusion, which is expressed in the touch receptor neurons AVM (QR.paa) and PVM (QL.paa) (Hamelin et al., 1992) and an X-gal-staining protocol that does not kill the eggs inside a stained hermaphrodite (Xie et al., 1995). EA23 *jeIn1[mec-7-lacZ+pRF4(rol-6d)]*; *pag-1(ls2)* hermaphrodites were mutagenized with ethyl methanesulfonate (EMS; Brenner, 1974). (*pag-1(ls2)* increases the intensity of *mec-7-lacZ* expression; Xie et al., 1995.) 3500 F_2 descendants from these animals were screened for the absence of a staining cell in the posterior where PVM is normally found.

egl-20(mu25) is an EMS-induced allele isolated in a screen using Nomarski optics to visualize animals with misplaced Q descendants. *egl-20(mu39)* was isolated in a screen for EMS-generated mutations affecting the expression of a *mab-5-lacZ* fusion gene, which will be described elsewhere (Maloof and Kenyon, unpublished data).

egl-20(mu27) was the only *egl-20* allele isolated in a non-complementation screen. EMS-mutagenized *him-5(e1490)* L4 males were mated to *unc-24(e138) egl-20(n585)* hermaphrodites. Approximately 2100 F_1 non-Unc L4 hermaphrodites were picked away from their male siblings, grown to adulthood and screened for the Egl phenotype. Their progeny were screened for a QL.(d) migration (Mig) defect. Since *unc-24(e138) egl-20(n585)/eDf19* are viable, fertile and Egl, we should have been able to identify and recover complete loss-of-function alleles in this screen.

48% of *mab-5(e2088)*/+; *egl-20(n585)*/+ animals have QL.pa daughters in anterior positions (i.e. in the V1-V3 region; n=56). To rule out the possibility that these new mutations were unlinked non-complementing mutations, we mapped *mu25*, *mu27* and *mu39* to the *egl-20* region, using *unc-24(e138)* and *dpy-20(e1282)* (see next section and data not shown).

Genetic mapping

egl-20. The *egl-20* gene maps to LG IV (Trent et al., 1983). We mapped *egl-20* between the genes *unc-24* and *dpy-20*. From heterozygotes of genotype *unc-24(e138)* + *dpy-20(e1282)*/+ *egl-20(n585)* +, 9/14 Dpy non-Unc recombinants and 8/20 Unc non-Dpy recombinants segregated Mig progeny. We also found that the deficiency *eDf19* failed to complement *egl-20(n585)* (data not shown).

mig-14. *mig-14(mu71)* was mapped to the right arm of LGII using STS markers (Williams et al., 1992). Three-factor mapping placed it

between *rol-1* and *unc-52*: from *rol-1(e91) unc-52(e444)/mig-14(mu71)* heterozygotes, 4/25 Rol non-Unc recombinants segregated Mig progeny. None of the known deficiencies in the region (*jDf1*, *jDf2*, *jDf4*) delete *mig-14*.

mig-1. Two-factor map data had placed *mig-1* on the left arm of LGI (Hodgkin et al., 1988). Three-factor mapping was used to further define the map position of *mig-1*. From heterozygotes of genotype + *lin-6(e1466) dpy-5(e61)/mig-1(e1787)* + +, 21/21 Dpy non-Lin recombinants segregated Mig animals. *lin-17*, whose QL.(d) cell mutant phenotype is similar to that of *mig-1* mutants, also maps to the left arm of LGI. However, deficiencies *tDf3* and *tDf4*, which delete the *lin-17* locus, both complement *mig-1(e1787)* (data not shown). Together, these data suggest that the map position of *mig-1* is near or to the left of *lin-6*, consistent with the two-factor map data, and confirm that *mig-1* and *lin-17* are two distinct genes.

Genetic analysis of gene activity

egl-20. Four of the five *egl-20* alleles, *n585*, *n1437*, *mu25* and *mu27*, have similar phenotypes at 20°C: severe QL descendant migration defects and HSN migration defects. At 25°C, *mu25* has a weaker QL descendant migration defect (see Table 1). The QL descendant migration defects are less severe in *egl-20(mu39)* mutants (see Table 1), which also fail to exhibit some of the other *egl-20* mutant phenotypes such as crumpled spicules, incomplete migration of rays 1 and 2 into the tail, and the A/P reversal of cells in the V5 lineage (data not shown).

We found that the *egl-20* allele *n585* is semi-dominant due to haploinsufficiency (Table 1) and behaves as a strong reduction-of-function mutation by genetic criteria. Placing the allele *n585* in *trans*

Table 1. Gene dosage analysis of *egl-20*: strong *egl-20* mutations are haploinsufficient for the QL descendant migration defect

Genotype	% QL desc. anterior	*n*
egl-20 (n585)	96%	50
mu27	100%	25
n1437	96%	36
mu25	83%	35
mu39	66%	25
eDf19/+	9%	123
egl-20 (n585)/+	7%	100
mu27/+	5%	114
n1437/+	3%	107
mu25/+	3%	181
mu39/+	0%	114
control +/+	0%	279

The positions of the QL.pa daughters were scored in L2 and late L1 larvae. Positions were scored as anterior if they were anterior to the V4.pp or V4.ppa nuclei in L2 or the posterior end of the V4.p nucleus in L1. *egl-20* heterozygotes were generated using the *unc-24(e138)* mutation to distinguish self- from cross-progeny (see Materials and Methods). The *eDf19* deficiency is maintained in *trans* to *unc-24(e138)* and *dpy-20(e1282)*. As a control, we examined *unc-24(e138) dpy-20(e1282)*/+ animals. *n*, number of animals scored for each genotype. The percentage of QL.pa daughters that migrate into the anterior in *egl-20* heterozygotes is significantly different from that of control animals according to the one-tailed Fisher Exact Test for all *egl-20* alleles except *mu39* (*eDf19*, $P<0.000002$; *n585*, $P<0.0001$; *mu27*, $P<0.0005$; *n1437*, $P<0.02$; *mu25*, $P<0.01$, *mu39*, $P<1.00$).

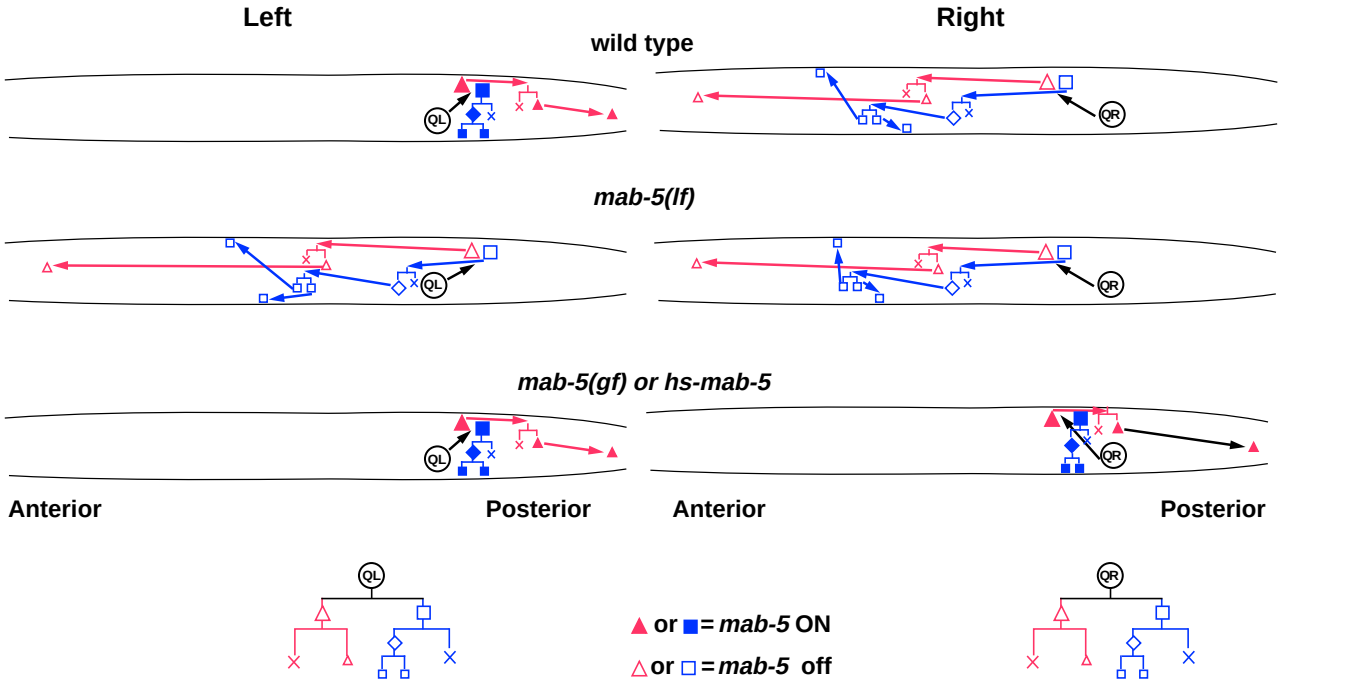

Fig. 1. Migration of the Q neuroblasts and their descendants in wild type (Sulston and Horvitz, 1977; Chalfie and Sulston, 1981), *mab-5(lf)* (Salser and Kenyon, 1992) and *mab-5(gf)* (Salser and Kenyon, 1992) mutants. Data are from Salser and Kenyon, (1992). Each cell in the lineage is denoted by a different shape (see lineage diagrams at bottom of figure): QL/R, circle; QL/R.a, large triangle; QL/R.ap (PQR/AQR), small triangle; QL/R.p, large square; QL/R.pa, diamond; QL/R.paa (PVM/AVM) and QL/R.pap (SDQL/R), small squares. Cells undergoing programmed cell death are marked with an x. Cell migrations are indicated by arrows. All cells divide and migrate along the A/P axis except for the daughters of the anteriorly migrating QR.pa cell, which also have a dorsoventral component to their migration. The divisions of cells other than QL or QR are symbolized by cell lineage diagrams. In all figures, anterior is to the left. Filled symbols indicate *mab-5* expression as determined by antibody staining (S. Salser and C. Kenyon, unpublished data; see also Fig. 4). This pattern is the same as that determined using *mab-5-lacZ* (Salser and Kenyon, 1992). The brief expression of MAB-5 in the QL neuroblast just before division is not depicted.

to a deficiency for the region, *eDf19*, did not increase the severity of the QL descendant defect, the HSN defect or the polarity reversal. These data suggest that the *n585* mutation may completely eliminate gene activity. In addition, placing the weak allele *mu39* in *trans* to either *n585* or *eDf19* increased the penetrance of the QL descendant and HSN migration defects to approximately the same degree. However, the polarity reversal phenotype was more severe in *mu39/eDf19* worms than in *mu39/n585* (data not shown). Thus the *n585* allele, although it is a strong reduction of function allele, may not represent the *egl-20* null phenotype.

To generate *egl-20* heterozygotes for gene dosage analysis (Table 1), hermaphrodites of genotype *unc-24(e138) egl-20* were crossed with N2 males, and their non-Unc progeny were scored. *eDf19* heterozygotes were identified as non-Unc, non-Dpy progeny from an *eDf19/unc-24(e138) dpy-20(e1282)* strain. As a control, *unc-24(e138) dpy-20(e1282)* hermaphrodites were crossed to N2 males and their non-Unc, non-Dpy progeny scored.

mig-14, mig-1* and *lin-17. The alleles of *mig-14*, *mig-1* and *lin-17* that we studied are all recessive (Ferguson and Horvitz, 1985; Desai et al., 1988; data not shown). Both alleles of *mig-14*, *mu71* and *k124*, have a QL descendant migration defect that is more than 95% penetrant (Fig. 3 and data not shown), although some of the other migration defects appear to be more severe in *k124* than *mu71* (K. Nishiwaki, personal communication and data not shown). The QL descendant migration defects in *mig-1* and *lin-17* mutants are less penetrant than those of *egl-20* and *mig-14* mutants, and some alleles of *mig-1* have no associated QL descendant migration defect at all. The positions of the QL.pa daughters are anterior to wild type in greater than 75% of worms homozygous for the *mig-1* alleles *e1787* (Fig. 3), *n687* and *mu72*, but less than 2% of worms homozygous for *n1354* and *n1652* (data not shown; Maloof and Kenyon, unpublished data). All *lin-17* alleles examined, *n671*, *n677* and *e1456*, have similar QL descendant migration phenotypes. However, the *lin-17(n671)* and *n677* mutations, reported to be the most severe *lin-17* alleles with respect to vulva formation (Ferguson and Horvitz, 1985), are both temperature sensitive for the QL descendant migration defect (data not shown). Interestingly, the *e1456* allele, reported to be weaker than *n671* and *n677* for other phenotypes (Ferguson and Horvitz, 1985), exhibits the migration defect at lower temperatures (data not shown). Thus, it is difficult to infer what the *lin-17* null phenotype might be and whether any of these alleles are null.

Since more than one allele of each of these genes caused a QL.(d) migration defect, the simplest explanation for all these mutations is that they reduce or eliminate gene function, and therefore function during normal development to activate *mab-5* expression in QL.

Scoring the positions of the Q.pa daughters

The positions of the Q.pa daughters were determined in late L1 after the descent of the last P nucleus into the ventral nerve cord. The positions of the QL descendants along the A/P axis were determined relative to those of the stationary Vn.p and Vn.a epidermal cells. QL/R.paa and its sister QL/R.pap migrate to nearby A/P positions and they are sometimes very close together. Since it was not always possible to determine which cell was which without observing the division of Q.pa, the positions of both cells were plotted on the same graphs. By convention, anterior is always to the left in all graphs and diagrams. All strains were examined at 25°C except *mig-14(mu71)*; *mab-5*(*e1751gf*), which was examined at 20°C.

Direct observation of Q lineage migrations

Worms were mounted for long-term observation as described by Sulston and Horvitz (1977). Unhealthy strains were observed at lower temperatures: *mig-1(e1787)* and *mig-14(mu71)*; *mab-5*(*e1751gf*) mutants at 20°C, and *mab-5(gf); egl-20(n585)* mutants at 22.5°C. All other strains were observed at 25°C.

Determination of Mab-5-like phenotypes

We examined *egl-20(n585)*, *mig-14(mu71)*, *mig-1(e1787)* and *lin-17(n671)* mutants at 25°C for other Mab-5 phenotypes (Kenyon, 1986). Tissues examined were: adult coelomocytes in hermaphrodites, and spicules, hooks and sensory rays 1-6 in males. More than 20 worms of each genotype were examined for each phenotype.

***egl-20, mig-14,* and *mig-1*.** All tissues examined were essentially wild type, except for two tissues in *egl-20* mutants: the coelomocytes, which were often missing (20/43), and the spicules, which were often crumpled (16/26).

lin-17. *lin-17* mutations are known to cause many asymmetric cell divisions to become symmetric or to adopt a reversed polarity. The lineage of the M mesoblast was abnormal in *lin-17* mutants (Sternberg and Horvitz, 1988); however, we found that 21 out of 25 animals produce adult coelomocytes, unlike *mab-5* mutants. Male tails have few rays, often with severely abnormal morphology (Hodgkin et al., 1988; and data not shown), but, unlike *mab-5* mutants, do not replace rays with alae (data not shown). *lin-17* mutations affect the formation of the hook and the organization of the spicules, as do mutations in *mab-5*; however, the defects in these structures are due to different developmental abnormalities in *lin-17* and *mab-5* mutants (Kenyon, 1986; Sternberg and Horvitz, 1988).

Antibody staining of whole-mount larvae

Larvae were fixed and stained with a rabbit polyclonal antisera to MAB-5 as described in Salser and Kenyon (1996). The DNA stain DAPI, which labels all nuclei, was used to confirm the identity of both *mab-5* immunoreactive and non-immunoreactive cells.

Single-cell activation of *hs-mab-5*

To induce *heat-shock-mab-5 (hs-mab-5)* expression in a migrating Q descendant, we heated it using a laser microbeam. Experiments were performed as described by Stringham and Candido (1993) with the modification that laser strength was calibrated daily by inserting neutral density filters in the laser light path until 15-25 pulses were needed to burst an *E. coli* cell. We then further attenuated the laser by placing a glued stack of 10 or 12 microscope slides perpendicular to the laser's path. The laser was focused on a single cell for 3 minutes at a pulse rate of 2.5 Hz. After testing several different integrated lines carrying *hs-mab-5*, we chose the strain CF301 *mab-5(e2088); unc-31(e169); him-5(e1490); muIs9[hs-mab-5 + C14G10(unc-31$^+$)]* (Salser et al., 1993) because of its high sensitivity and low background in whole-animal heat shocks. Animals were kept at 20°C throughout the experiments. 3.5-4 hour old L1 larvae were mounted on agarose pads containing 2 mM azide to immobilize them. After laser treatment, animals were allowed to recover for 1 hour on a seeded NG plate and then were remounted on agarose pads. The migrating cells were followed until QR.a or QR.ap had remained stationary for at least 2 hours, usually about 8 hours total. Reversals were defined as migrations in which QR.a or QR.ap moved towards the posterior and passed more than one nucleus in the surrounding epidermis. The data presented in Fig. 2 represents all experiments carried out once conditions were found that caused QR.a migration reversals. To insure that the reversals were dependent on the laser heat shock of QR.a, we carried out controls in parallel in which animals were mounted on azide for the same amount of time but without laser pulsing. Controls in which QR.a was targeted in N2 (wild-type) worms were also done in parallel. We found that the laser intensity necessary for inducing QR.a reversals had the side effect of delaying or blocking the division of QR.a. This effect was independent of *mab-5*, however, because focusing the laser on QR.a in wild-type worms also delayed or blocked the division but did not induce reversals. We did not test the effect of laser induction of *mab-5* in QR.p and QL.p because *mab-5* expression in this branch of the QL and QR lineage causes these cells to stop migrating (Fig. 1), a result indistinguishable from that caused by cell damage.

RESULTS

Wild-type Q lineage migrations

The QR and QL neuroblasts are born at the same time, in the same A/P position on opposite sides of the animal (Sulston and Horvitz, 1977). These cells each undergo an identical sequence of divisions (Fig. 1) to produce one mechanosensory neuron (AVM/PVM), one putative interneuron (SDQR/SDQL), a ciliated neuron (AQR/PQR) and two cells that undergo programmed cell death (Sulston and Horvitz, 1977; Chalfie and Sulston, 1981; White et al., 1986). Approximately one hour after the worm hatches, QL and QR begin their migrations: QL towards the tail and QR towards the head. After these initial migrations, QL and its descendants activate expression of the Hox gene *mab-5*. The *mab-5*-expressing cells then remain in the posterior: QL's posterior daughter, QL.p, and its descendants stop migrating, while QL's anterior daughter, QL.a, and its descendant continue migrating towards the posterior. In contrast, QR and its descendants do not express *mab-5* (Salser and Kenyon, 1992) and migrate towards the anterior (Fig. 1).

In mutants lacking *mab-5* activity, the initial migrations of QL towards the tail and QR towards the head are unaffected, but the descendants of both QL and QR migrate towards the head, just as the descendants of QR do in wild type (Fig. 1) (Kenyon, 1986; Salser and Kenyon, 1992). In animals that express *mab-5* ectopically, such as *mab-5(gf)* mutants (Hedgecock et al., 1987; Salser and Kenyon, 1992) or animals carrying *heat-shock-mab-5* (Salser and Kenyon, 1992), the initial migration of QR is still towards the head, but now QR.p and its descendants stop and QR.a and its descendants migrate towards the tail, just as QL.p, QL.a and their descendants do in wild type (Fig. 1). In this paper, we will refer to the daughters of QL and QR and all of their subsequent descendants collectively as QL.(d) and QR.(d) cells.

Previous mosaic analysis has shown that *mab-5* activity is required within the AB.p branch of the *C. elegans* lineage for QL's descendants to migrate posteriorly (Kenyon, 1986). Since QL is derived from AB.p, this finding is consistent with the cell autonomous action of *mab-5*. This interpretation is strengthened by the observation that *mab-5* expression is activated in QL, but not QR (Salser and Kenyon, 1992). However, the possibility remained that *mab-5* activity in some other AB.p descendant, such as V3, V5 or the P cells, might influence the QL.(d) migrations. Therefore, to ask whether *mab-5* activity within a migrating Q.(d) cell is sufficient to direct its posterior migration, we used an attenuated laser microbeam to activate *hs-mab-5* within a single cell (see Materials and Methods). We found that focusing the laser beam on the anteriorly migrating QR.a cell, but not surrounding cells, caused QR.a to reverse direction and migrate towards the posterior (Fig. 2).

Despite the fact that in wild-type animals all three QL-derived neurons express *mab-5*, each cell comes to occupy a characteristic position along the body axis (Fig. 1). Similarly, all three QR-derived neurons fail to express *mab-5*, yet each of them migrates to a different characteristic position (Fig. 1). Thus, although *mab-5* expression plays an important role in determining whether these cells ultimately reside in the posterior or the anterior of the body, it does not appear to be sufficient to specify their precise locations.

Genes affecting Q descendant migration: Overview

In this paper, we describe four genes that affect the migrations of the Q.(d) cells along the A/P body axis. A number of mutants had been identified previously in which the descendants of QL were located in anterior body regions (*mig-1*: Hedgecock et al., 1987; *lin-17*: Way et al., 1992; *egl-20*: G. Garriga, personal communication), and we identified additional mutants with this phenotype (Fig. 3A; see Materials and Methods). Mutations in three of these genes were previously identified on the basis of other mutant phenotypes: *egl-20* mutants are **Eg**g-**l**aying detective, *mig-1* mutants have other **Mig**ration defects and *lin-17* mutants are **Lin**eage abnormal. Mutations in *egl-20*, *mig-1*, *mig-14* and *lin-17* can cause the QL.(d) cells, which normally migrate posteriorly, to reverse direction and migrate anteriorly instead. In addition to their effect on the direction of migration, mutations in two of these genes, *egl-20* and *mig-14*, affect a second aspect of cell positioning of both the QL.(d) and QR.(d) cell migrations: namely, that subsequent anterior migrations are shortened and posterior migrations are lengthened. We will discuss these two different mutant phenotypes in turn, beginning with the change in direction of migration.

Mutations in *egl-20*, *mig-1*, *mig-14* and *lin-17* reverse the direction of migration of QL's descendants

The QL.(d) cells in *egl-20*, *mig-1*, *mig-14* and *lin-17* mutants migrate towards the anterior just as they do in *mab-5* mutants (Fig. 3A). Are these reversals due to a failure of the *mab-5* switch? *mab-5* mutations do not affect the initial posterior migration of QL, only that of the descendants. Thus, if *mab-5* activity in QL were blocked, one would expect QL to migrate posteriorly, but its descendants to migrate anteriorly, as they do in *mab-5* mutants (Fig. 1). To ask whether QL migrated posteriorly in these mutants, we observed its migration in living animals using Nomarski microscopy. We found that, in these mutants, QL initially migrated towards the posterior, the same trajectory observed in wild type, but its descendants migrated towards the anterior, as in *mab-5(–)* mutants (Fig. 3B). Thus, these four genes, *egl-20*, *mig-1*, *mig-14* and *lin-17*, were likely to function in the *mab-5* pathway.

Mutations in *egl-20*, *mig-14*, *mig-1* and *lin-17* prevent MAB-5 expression in QL

In principle, the QL.(d) cells could migrate anteriorly in these mutants either because they fail to express *mab-5*, or because they fail to respond correctly to *mab-5*. To distinguish between these two possibilities, we first used polyclonal antisera against *mab-5* protein (MAB-5) (Salser et al., 1993) to determine whether QL and its daughters, QL.a and QL.p, produced MAB-5. We found that although QL.a and QL.p always expressed *mab-5* strongly in wild-type worms, they produced no detectable MAB-5 in *egl-20(n585)* and *mig-14(mu71)* mutants (Fig. 4; Table 2).

The effect on *mab-5* expression at this stage seemed to be fairly specific for QL.a and QL.p: surrounding cells (V6, P9/10, P11/12, M and the seven most posterior juvenile motoneurons) appeared to produce MAB-5 as in wild type (data not shown). We also found that, in general, *mab-5*-dependent cell fates in four other tissues (the hermaphrodite M-derived coelomocytes, male spicules, rays 1-6 and hooks)

A.

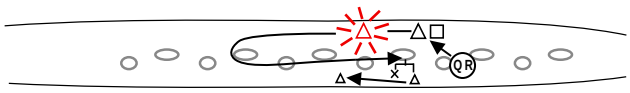

B.

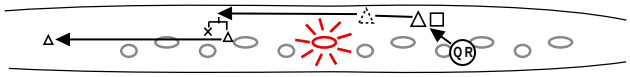

C.

genotype	targeted cell	QR.a reversed
hs-mab-5	QR.a	18/38
"	"nearby" epidermal cell (V3)	0/9
"	"distant" epidermal cell (V1,V2,V6, or P1-2)	0/8
"	dorsal syncytial nucleus	0/5
"	QR.p	0/2
"	none (mock treatment)	0/17
wild type	QR.a	0/16

Fig. 2. Laser activation of *hs-mab-5* in QR.a as it migrates anteriorly causes the cell to reverse direction and migrate posteriorly. During the anterior migrations of QR.a and QR.p, an attenuated laser beam was focused on a single nucleus for three minutes in order to activate *mab-5* expression, and the resulting cell migrations were observed during the following 8-10 hours (see Materials and Methods). The symbols indicating cells in the QR lineage are the same as those in Fig. 1. The QR.p lineage (square) was unaffected and is omitted. Gray ovals show Vn.a and Vn.p epidermal cells and correspond to the horizontal axis of Figure 3. The targeted cell is indicated with radiating lines. (A) Sample lineage from a *mab-5(e2088); muIs9(hs-mab-5)* animal in which the laser was focused on QR.a (red triangle). QR.a continued to migrate anteriorly, then reversed direction and migrated toward the posterior, divided as QR.a normally does, and then migrated a short distance to the anterior (presumably due to decay of the *hs-mab-5* activity (Salser and Kenyon, 1992). (B) Sample lineage from *mab-5(e2088); muIs9(hs-mab-5)* animal in which the laser was focused on a nearby cell, V3.p. At that time, QR.a (dashed triangle) was just dorsal of V3.p but was unaffected, continuing its normal anterior migration pattern. (C) Summary of all laser heat-shock experiments. In all cases, the laser was focused on cells on the right side of the animal during the time that QR.a was migrating anteriorly (between V3 and V4). The targeted 'nearby' epidermal cells were: V3, V3.a and V3.p (n=3, 2 and 4, respectively). 'Distant' epidermal cells were: V1, V2, V2.a, V2.p, V6 and P1/2 (n= 1, 1, 1, 1, 2 and 2, respectively). Dorsal syncytial nuclei were: the hyp7 nucleus between V2 and V3 (n=4) and the hyp7 nucleus between V1 and V2 (n=1). Using the positions of the Vn.a and Vn.p cells as a ruler (see horizontal axis for Fig. 3, in which each tick mark is defined as one unit) the distance migrated toward the posterior in the QR.a reversals ranged from 4 to 13 units, mean = 7.9.

(Kenyon, 1986) were normal in *egl-20*, *mig-14* and *mig-1* mutants (exceptions are described in Materials and Methods). These tissues were defective in *lin-17* mutants, but had a phenotype that differed from that of *mab-5* mutants (see Materials and Methods). Therefore these genes are not required globally for *mab-5* expression.

When we examined MAB-5 expression in *mig-1(e1787)* and *lin-17(n671)* mutants, we found that the QL daughters showed decreased MAB-5 staining in 83% of *mig-1* mutants and 48% of the *lin-17* mutants (Fig 4; Table 2). As in *egl-20* and *mig-14* mutants, staining appeared normal in surrounding cells. Since these *mig-1* and *lin-17* mutants have an incompletely penetrant migration defect, the QL.(d) cells that remain in the posterior in *mig-1* mutants could do so as a result of *mab-5* activity. To test this, we removed *mab-5* activity using a *mab-5* null mutation, *e1239* (Salser and Kenyon, 1996). We found that the QL.pa daughters were located in full anterior positions (anterior to V3.a) in 98% (n=67) of the *mig-1*(*e1787*); *mab-5*(*e1239*) double mutants. The same was true for *lin-17(n671); mab-5(e1239)* double mutants constructed and analyzed previously by Way et al. (1992). These observations indicate that the QL descendants that remain in the posterior, or in intermediate positions, in *mig-1* and *lin-17* mutants do so largely as a result of *mab-5* activity.

If the QL.(d) cells in *mig-1* and *lin-17* mutants migrate incorrectly because they fail to express MAB-5, then they would be expected to migrate correctly if provided with MAB-5. To test this, we used a *mab-5* gain-of-function mutation, *e1751gf*, a regulatory mutation that causes ectopic production of MAB-5 (Salser and Kenyon, 1992; Salser et al., 1993). In *e1751gf* mutants, both QL and QR produce MAB-5, and both the QL and QR descendants migrate to posterior positions (Hedgecock et al., 1987; Salser and Kenyon, 1992) (Fig. 5). We found that in double mutant combinations between *mab-5(e1751gf)* and *egl-20*, *mig-1* or *mig-14* mutations, the QL.pa descendants remained in the posterior (Fig. 5). This shows that the QL.(d) cells in *egl-20*, *mig-1* and *mig-14* mutants can respond correctly to MAB-5. This finding, together with the MAB-5 expression data, indicates that the QL.(d) cells migrate towards the anterior in *egl-20*, *mig-1* and *mig-14* mutants because they fail to express MAB-5.

We were unable to maintain *lin-17*(*n671*); *mab-5(e1751gf)* double mutants because the animals were very sick. However, the frequency of QL daughters in *lin-17* mutants that have little or no MAB-5 staining correlates well with the percentage of QL descendants that migrate into the anterior, as it does for *mig-1* mutants (Table 2), and the QL.(d) cells that remain in the posterior require *mab-5* activity to do so (Way et al., 1992). Together, these observations suggest that a lack of *mab-5* expression in the QL.(d) cells causes them to migrate into the anterior.

In *egl-20* and *mig-14* mutants the anterior migrations of the QR descendants are shortened

In addition to their failure to express *mab-5* in QL, *egl-20* and *mig-14* mutants also exhibit a second migration phenotype. In the wild type, the three QR-derived neurons each stop at unique and characteristic positions in the anterior, just as the three QL-derived neurons do in the posterior. Interestingly, we found that, in *egl-20* and *mig-14* mutants, but not *mig-1* and *lin-17* mutants (data not shown),

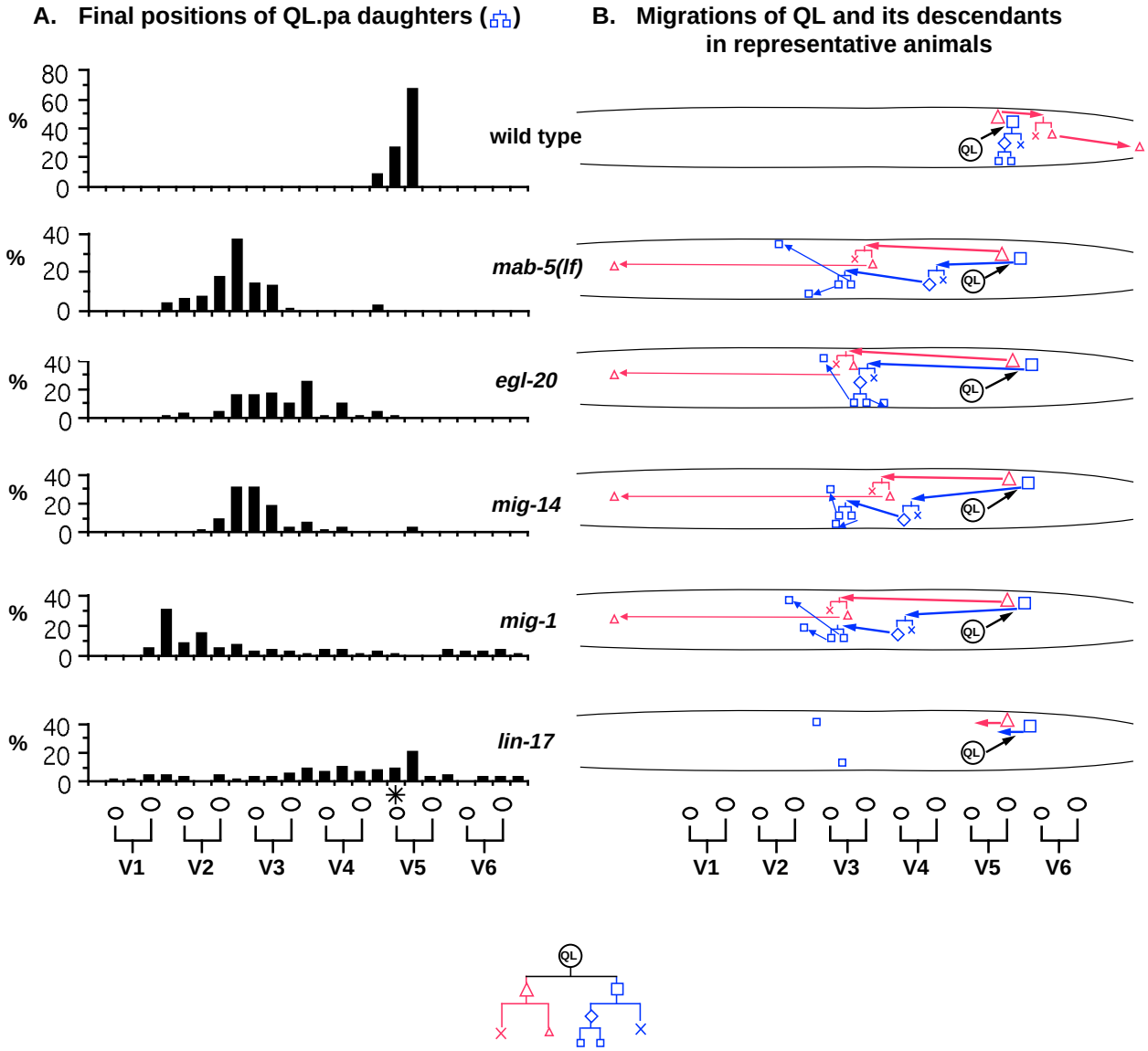

Fig. 3. The migrations of the QL descendants in wild-type and *mab-5(e2088)*, *egl-20(n585)*, *mig-14(mu71)*, *mig-1(e1787)* and *lin-17(n671)* mutants. The positions of the QL descendants along the A/P axis were determined relative to that of the stationary Vn.a and Vn.p epidermal cells, shown at the bottom of the figure (see Materials and Methods). (A) Final positions of the QL.pa daughters, AVM and SDQL, at 25°C. The asterisk above V5.a marks the birthplace of QL. 50 animals of each genotype were scored. (B) The migrations of QL and its descendants in representative animals of each genotype. The migrating cells were followed in living animals using Nomarski (DIC) optics. The different cells are depicted by different shapes (see lineage diagram at bottom of figure) as described in Fig. 1. The cells in the Q.p branch of the lineage are labelled blue and in the Q.a branch are labelled orange. We observed the complete migrations in 5 *egl-20*, 3 *mig-14* and 4 *mig-1* mutants. Data for wild-type and *mab-5* mutant migrations are from Salser and Kenyon (1992). Illustrated lineages are representative. The following variation was seen: (***egl-20***). QL.p did not migrate at all in one *egl-20* mutant, although its daughter, QL.pa, did. QL.pa migrated anteriorly in 3/5 animals and did not migrate at all in the other two. In one animal, QL.ap did not migrate into the head but stopped in the body, just posterior to V1.p. In addition, in one animal, the polarity of the QL.a division was reversed: QL.aa migrated and QL.ap died. The migration of QL.aa in this animal was quite unusual; first it migrated anteriorly past three nuclei, then changed direction and migrated posteriorly past four nuclei, then changed direction again and migrated anteriorly past seven nuclei to a position just adjacent to V3.a, where it stopped. (***mig-14***). In one animal QL.ap did not migrate into the head, but stopped in the body between V1.a and V1.p. (***mig-1***). In one *mig-1* mutant the QL.(d) cells migrated as in wild type. (***lin-17***). *lin-17* mutants were not observed continuously, since their development at 25ºC, where the Mig defect is observed, is greatly retarded. Instead, the initial migration of QL was observed and then the final positions of the QL.pa descendants were scored the following day. In all 8 *lin-17* mutants examined, QL migrated towards the posterior; in four of those animals the QL.pa daughters migrated to positions anterior to wild-type.

the final positions of most of the QR.pa daughters were consistently shifted posteriorly relative to wild type (Fig. 6, column 1). When we observed the QR.(d) migrations in living animals using Nomarski microscopy, we found that, in general, these cells stop migrating prematurely (Fig. 7A). We also noticed a similar alteration in the QL.(d) migrations: for

example, in *egl-20* or *mab-5; egl-20* double mutants, the final positions of these cells were generally shifted significantly posteriorly relative to the positions in the anterior that they would come to occupy in *mab-5(lf)* mutants (Fig. 3 and data not shown). Since the anterior-directed QL.(d) migrations of *egl-20* and *mig-14* mutants are shorter than those of *mab-5(lf)* mutants, the *egl-20* and *mig-14* mutant phenotypes cannot be completely explained by a loss of *mab-5* expression in the

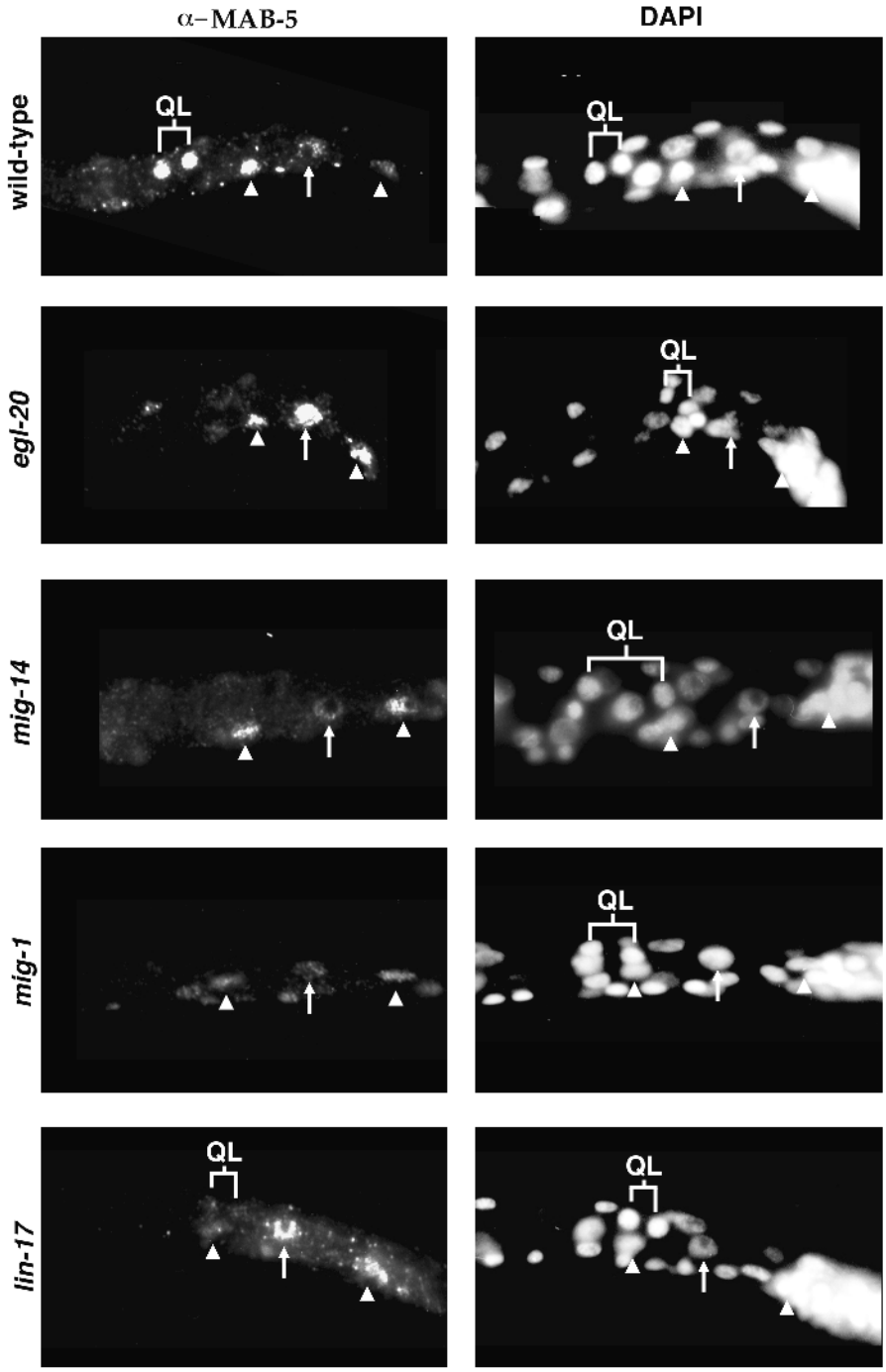

Fig. 4. MAB-5 expression in QL.a and QL.p. Whole-mount larvae, 3-6 hours post-hatching (raised at 25°C), were stained with polyclonal anti-MAB-5 antisera and the DNA stain DAPI (Salser et al., 1993). At this time, QL has just divided and both daughters stain brightly with anti-MAB-5 antisera in wild type (top panels). In the *egl-20, mig-14* and *mig-1* mutants depicted above, QL.a and QL.p did not stain with anti-MAB-5 antisera. The *lin-17* mutant shown here demonstrates the faint MAB-5 staining occasionally seen in QL.a and QL.p in *mig-1* and *lin-17* mutants. Some other MAB-5-immunureactive cells are labeled for reference: arrow indicates V6, left arrowhead indicates P9/10, right arrowhead indicates P11/12.

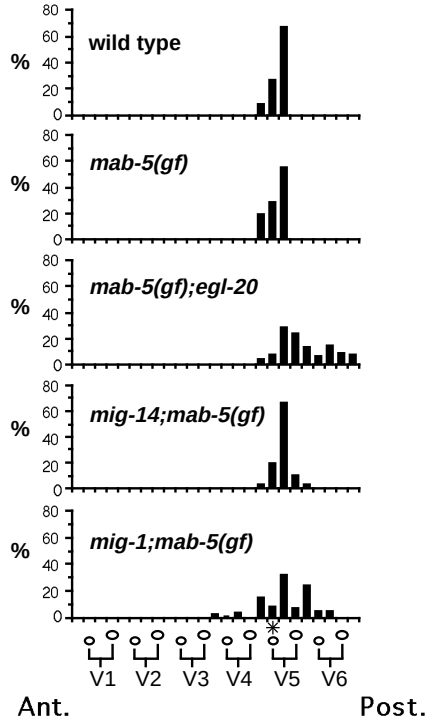

Fig. 5. A *mab-5(gf)* mutation suppresses the anterior migrations of the QL.(d) cells in *egl-20*, *mig-14* and *mig-1* mutants. Final positions of the QL.pa daughters (small blue squares in Figs 1 and 3) in worms carrying *mab-5(e1751gf)* alone and in combination with *egl-20(n585)*, *mig-14(mu71)* and *mig-1(e1787)*. The positions in wild type are shown for comparison. The star above V5.a marks the birthplace of QL. *n*=35 for *mig-14; mab-5(gf)*. *n*=50 for all other genotypes. In *egl-20*, *mig-14*, *mig-1* and *lin-17* mutants, but not in *mab-5* mutants, the migration of QL towards the posterior was lengthened, so that it divided next to P9/10 or even V6 instead of dividing over V5 (see positions of QL.a and QL.p in Fig. 4). *egl-20* L1 larvae are slightly Dumpy, so distances between cells are shorter, but the other three mutants are of normal length. The lengthened QL migration may be responsible, at least in part, for the QL.pa daughters that are posterior to wild type in *mab-5(e1751gf)* double mutants (shown here), and in the *mig-1* and *lin-17* mutants that have sufficient *mab-5* activity to remain in the posterior (Fig. 3).

Table 2. Correlation of MAB-5 expression in QL.a and QL.p with posterior positions of the QL.pa daughters

	(A) *mab-5* Ab staining in QL.a and QL.p				(B) Position of QL.pa desc.	
Genotype	% bright	% faint	% none	(*n*)	% posterior	(*n*)
wild type	98	2	0	(94)	100	(50)
egl-20(n585)	0	0	100	(27)	4	(50)
mig-14(mu71)	0	0	100	(31)	2	(50)
mig-1(e1787)	17	11	72	(72)	15	(50)
lin-17(n671)	52	27	21	(52)	48	(50)

n, number of sides scored. All worms were grown at 25°C. (A) The percentage of worms with QL.a and QL.p staining brightly with antisera to MAB-5 (see Materials and Methods). All worms were fixed at 3-6 hours after hatching except for *mig-14* mutants which were fixed at 3.5-4.5 hours. Staining was only scored in animals in which QL had divided. (B) The percentage of animals in which the final position of the QL.pa descendants at the end of L1 was posterior to V4.p. Data taken from Fig. 3.

We did not examine *mab-5* expression and final position in the same animals since *mab-5*-expressing QL.(d) cells, which migrate into the anterior stop expressing *mab-5* (Salser and Kenyon, unpublished data). Thus we scored *mab-5* expression in QL.a and QL.p before they had migrated very far.

QL lineage. Because *egl-20* and *mig-14* influence *mab-5* expression as well as this additional aspect of cell position in the QL lineage, in the following sections, we will describe the shortening of the anterior migrations on the right side only, where cells in the QR lineage do not express *mab-5*.

The shortening of the anterior migrations of the QR descendants in *egl-20* and *mig-14* mutants is not due to a defect in motility

What causes the QR descendants to stop short in *egl-20* and *mig-14* mutants? These cells may be specifically defective in anterior migration, or they may simply be unable to migrate well in any direction. Alternatively, these mutations may direct cells to migrate to positions shifted posterior to normal. To distinguish between these possibilities, we asked what effect *egl-20* or *mig-14* mutations would have on a mutant in which QR.p did not migrate at all. In worms carrying the *mab-5* gain-of function mutation, *e1751gf*, QR.p and its descendants do not migrate and QR.a and its daughter migrate towards the posterior (Fig. 7). We found that, when an *egl-20* or *mig-14* mutation was introduced into this strain, the QR.p cell now migrated towards the tail (Fig. 7), thus shifting

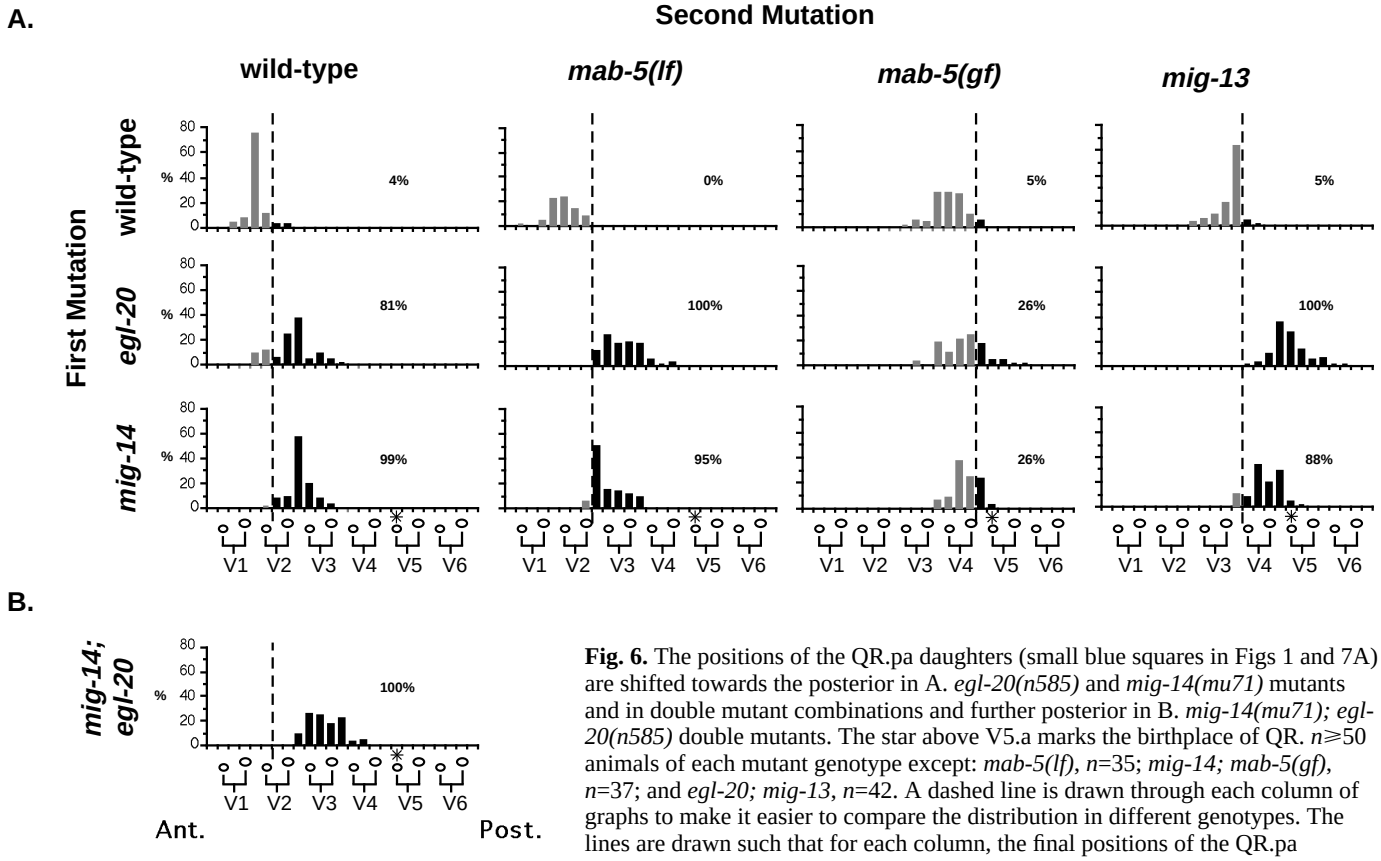

Fig. 6. The positions of the QR.pa daughters (small blue squares in Figs 1 and 7A) are shifted towards the posterior in A. *egl-20(n585)* and *mig-14(mu71)* mutants and in double mutant combinations and further posterior in B. *mig-14(mu71); egl-20(n585)* double mutants. The star above V5.a marks the birthplace of QR. $n \geqslant 50$ animals of each mutant genotype except: *mab-5(lf)*, $n=35$; *mig-14; mab-5(gf)*, $n=37$; and *egl-20; mig-13*, $n=42$. A dashed line is drawn through each column of graphs to make it easier to compare the distribution in different genotypes. The lines are drawn such that for each column, the final positions of the QR.pa daughters in 95% or more of control worms (top histogram of each column) are anterior to this line. The percentage of worms of each genotype with QR.pa descendants posterior to the line are noted at the right of each histogram. The QR.pa daughters in *egl-20* and *mig-14* mutant strains (second and third rows of A) are significantly different from that of control strains (top row of A) according to both the Kruskal-Wallis test and Sheffe's test ($P<0.0001$).

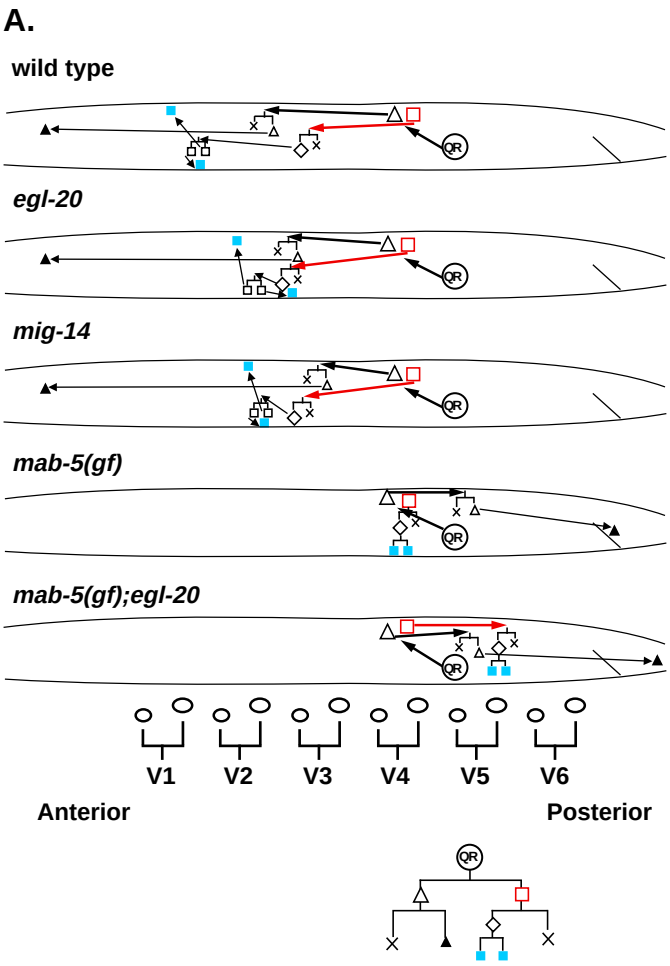

Fig. 7. The migrations of QR and its descendants. The migrating cells were observed using Nomarski (DIC) optics. (A) QR lineage migrations in representative wild-type and mutant worms. Cells in the lineage are denoted by different shapes, as described in Fig. 1 (see lineage diagram at bottom of Part A). The final positions of the QR.pa daughters are labelled blue. The QR.p cell and its migration are labelled red. We observed the complete migrations in two *egl-20*, three *mig-14* and three *mab-5(gf); egl-20* mutants. The data for the wild-type and *mab-5(gf)* mutant migrations are taken from Salser and Kenyon (1992). Diagonal line near tail marks the position of the anus. (B) The migrations of QR.p (red square and arrow in part A) in wild-type and mutant animals. Each arrow represents the migration of QR.p in a different animal. Only cells that passed both a Vn.a/p nucleus and an internuclear interval were defined as having migrated. QR.p cells that did not migrate are indicated with a red circle. The asterisk above V5.a marks the birthplace of QR. The dashed line is for reference and marks the average birthplace of QR.p.

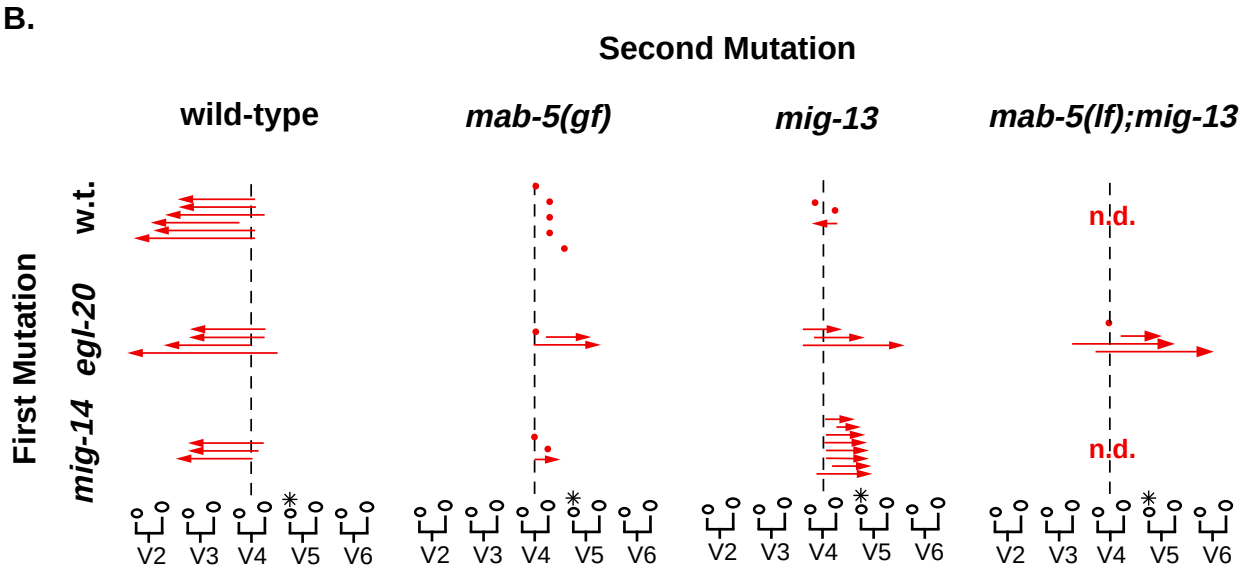

the positions of the QR.pa daughters towards the posterior (Fig. 6, column 3). This meant that a loss of *egl-20* or *mig-14* activity could cause a normally stationary cell to migrate posteriorly. We also observed that in *mab-5(gf); egl-20* double mutants, QR.a and its daughter, QR.ap, now migrated further posteriorly than in the *mab-5(gf)* single mutant (Fig. 7A, black triangles). These new findings are not consistent with the hypothesis that *egl-20* mutants are defective in cell motility. Instead, they imply that *egl-20* and *mig-14* mutations cause cells to migrate to positions located posterior to their normal stopping points.

In another mutant, *mig-13(mu31)*, QR.p and its descendants

only migrate a short distance to the anterior (Robinson, 1995; Fig. 7B). The *mu31* mutation is recessive and the severity of the phenotype does not increase in *trans* to a deficiency (Robinson, 1995). Thus, the wild-type function of *mig-13* is probably to allow QR.(d) cells to migrate anteriorly. Since mutations in *egl-20* and *mig-14* shift the positions of the QR.pa daughters toward the posterior in wild-type, *mab-5(lf)* and *mab-5(gf)* mutants, we wondered whether they would shift the QR.pa daughters towards the posterior in a *mig-13* mutant as well: specifically, might they cause the QR.p cell to actually reverse direction and migrate posteriorly? We found that the positions of the QR.pa daughters in *mig-13* mutants carrying *egl-20* or *mig-14* mutations were consistently shifted posterior relative to the *mig-13* single mutants (Fig. 6, column 4), and some, most strikingly in the *egl-20; mig-13* double mutant, were actually posterior to the birthplace of QR (denoted by asterisks at the bottom of Fig. 6). We followed the migrations of QR and its daughters in both *egl-20; mig-13* and *mig-14; mig-13* double mutants and found that QR.p always migrated in the reverse direction, towards the posterior, whereas, in *mig-13* single mutants, QR.p either stopped or migrated towards the anterior (Fig. 7B). These observations indicate that loss of *egl-20* or *mig-14* activity can cause a QR.(d) cell to change its direction of migration from anterior to posterior.

In the wild type, posterior migration of Q.(d) cells requires *mab-5* activity. Is *mab-5* required for the posterior migration caused by *egl-20* mutations? To ask whether the posterior migration of these cells required *mab-5* activity, we constructed and analyzed *mab-5(e2088); egl-20(n585); mig-13(mu31)* triple mutants. We found that, in these mutants, QR.p migrated towards the posterior in 3 out of 4 animals (Fig. 7B). This observation indicates that *mab-5* is not absolutely required for posterior migration.

The known Hox gene functions are not responsible for the shortened migrations of the QR descendants in *egl-20* and *mig-14* mutants

Both *egl-20* and *mig-14* mutations affect the expression of the Hox gene *mab-5*. Could the posterior shift in the positions of the QR.pa daughters in *egl-20* and *mig-14* mutants be explained by altered activities of the Hox genes? Of the four *C. elegans* Hox genes, three, *lin-39*, *mab-5* and *egl-5*, are known to be required for wild-type Q.(d) migrations (Kenyon, 1986; Costa et al., 1988; Chisholm, 1991; Clark et al., 1993; Wang et al., 1993). There are no mutations in the fourth gene, *ceh-13*, and its function is unknown (Shaller et al., 1990; Wang et al., 1993).

The Hox gene *lin-39* is required for patterning the central body region and for the anterior migrations of QR and its descendants (Clark et al., 1993; Wang et al., 1993). In *lin-39* mutants, the anterior migrations of QR and its descendants are shortened. To determine whether reduced *lin-39* activity in *egl-20* and *mig-14* mutants is responsible for shortening anterior QR.(d) migrations, we first examined the expression of a *lin-39-lacZ* fusion gene (Wang et al., 1993) in *egl-20* and *mig-14* mutants. *lin-39-lacZ* is normally expressed in both QL and QR (Wang et al., 1993) and we found that its expression in both cells was unaffected by *egl-20* or *mig-14* mutations (data not shown). Second, we examined the QR.(d) migrations in a double mutant containing *egl-20(n585)* and a *lin-39* null allele, *mu26* (Wang et al., 1993; J. Maloof and C. Kenyon, unpublished data). If the shortened anterior migrations of the QR.(d) cells in *egl-20* mutants were due to a loss of *lin-39* activity, then the migrations in the *lin-39*; *egl-20* double mutant should be the same as those in the *lin-39* single mutant. We found that the positions of the QR.pa daughters in the double mutant were further posterior than in the *lin-39(mu26)* single mutant (data not shown). Since the presence of an *egl-20* mutation shortened the anterior-directed migrations of the QR.(d) cells in a *lin-39* null mutant, the failure of these cells to migrate to their normal positions in *egl-20* mutants cannot be explained simply by a loss of *lin-39* activity.

Another possibility is that the QR.(d) cells did not migrate as far anteriorly as normal because they misexpressed the Hox genes *mab-5* or *egl-5*. These two genes are required for the posterior migrations of the QL.(d) cells: *mab-5* activity is required in all animals (Kenyon, 1986; Salser and Kenyon, 1992) whereas *egl-5* activity is required in approximately 9% of wild-type animals (Chisholm, 1991). To test whether ectopic *mab-5* or *egl-5* activity could be responsible for the shortened anterior migrations and lengthened posterior migrations of the QR descendants in *egl-20* and *mig-14* mutants, we made double mutants between *mab-5(e2088)* or *egl-5(n945)* and *egl-20(n585)* or *mig-14(mu71)*. We found that neither Hox mutation rescued the shortened QR.(d) migrations of *egl-20* and *mig-14* mutants (Fig. 6 and data not shown). These observations demonstrate that the posteriorly shifted positions of the QR.pa daughters in *egl-20* and *mig-14* mutants are not due to ectopic *mab-5* or *egl-5* activity.

The phenotypes of mutations in *egl-20* and *mig-14* are additive

We examined the positions of the QR.pa descendants in *mig-14(mu71); egl-20(n585)* double mutants, and found that they were shifted even further posterior than either single mutant (Fig. 6B). Further genetic and molecular analysis of these alleles should help us to determine whether these genes function in the same or in parallel pathways to determine the stopping points of the migrating QR.(d) cells.

Effect of *egl-20*, *mig-14*, *mig-1* and *lin-17* mutations on other cell migrations

To ask whether these mutations affected other cell migrations, we examined the positions of the migratory cells HSN, ALM, CAN, muIntR, ccLa/p, ccRa/p and M (Fig. 8). Mutations in *egl-20*, *mig-14*, *mig-1* and *lin-17* affected a few migrating cells but did not produce a consistent posterior shift. Since we have not examined the position of every cell in these mutants, the possibility remains that *egl-20*, *mig-14*, *mig-1* and *lin-17* may also play a broader role in cell migration than we have so far determined.

DISCUSSION

Our experiments address two important questions: First, what initiates expression of a Hox gene in a migrating cell, and second, what directs migrating cells to their final positions? We have identified four genes required to activate *mab-5* in QL (Fig. 9A). Two of these genes, *egl-20* and *mig-14*, are also required independently of *mab-5* activity to position the

A.

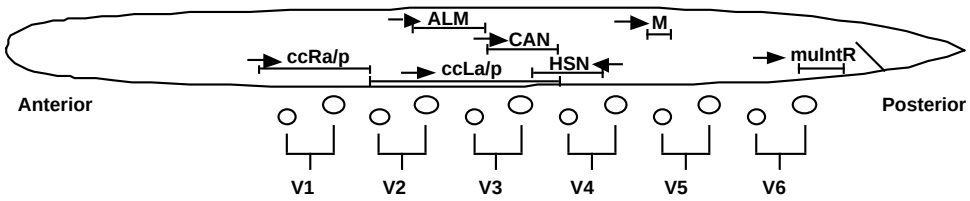

B.

Mig. Cells	% misplaced (n) wild type	*egl-20(n585)*	*lin-17(n671)*	*mig-1(e1787)*	*mig-14(mu71)*
HSN	4% (99)	81% (98) p	18% (77) a,p	38% (97) p	95% (43) p
ALM	0% (50)	5% (38)	10% (21)	2% (40)	26% (50) p
CAN	8% (50)	5% (40)	0% (22)	0% (40)	2% (50)
muIntR	0% (40)	2% (42)	0% (40)	6% (31)	0% (25)
ccLa/p	0% (38)	10% (47)	6% (40)	10% (40)	4% (23)
ccRa/p	3% (43)	18% (41) a	10% (41)	10% (40)	6% (33)
M	18% (34) a	68% (34) a	20% (40) a,p	35% (31) p	40% (25) a

Fig. 8. Other cell migrations in wild-type and mutant worms. Cell positions in N2 at 20°C are defined as wild type (data not shown). (A) The final positions of migratory cells in wild-type worms at 20°C. Range of final positions indicated beneath cell name was determined by examining more than 20 worms. Each worm has two HSN, ALM and CAN neurons, one per side, but only one M and muIntR cell, both found on the right side (Sulston and Horvitz, 1977). There are also two pairs of juvenile coelomocytes found in different A/P positions (Sulston and Horvitz, 1977): ccLa/p on the left side and ccRa/p on the right side. Final positions of all cells were determined relative to the positions of the Vn.p and Vn.a cells (bottom of A) except for M and muIntR, which were determined relative to the positions of the undivided V and P cells and then extrapolated onto this diagram of a later developmental stage. The migrations of all these cells occur during embryogenesis, prior to Q cell migration. Arrows indicate direction of migration. Diagonal line near tail marks the position of the anus. (B) The percentage of worms grown at 25°C which have misplaced migratory cells. Note the effect of temperature on some migrations in wild-type animals. n, number of sides scored; a, mostly anterior to wild type; p, mostly posterior to wild type. The HSN position observed in *egl-20* and *mig-1* mutants at 25°C is similar to that previously observed in worms grown at 20°C (Garriga et al., 1993). The position of M is unaffected by mutations in *mab-5* (data not shown). **Other migration defects.** In addition to the defects described above, all four mutants have variable defects in the migrations of the distal tip cells (Kiyoji Nishiwaki, personal communication and J. H., L. H., N. R. and C. K., unpublished data). Also, in *mig-14(mu71)* mutants, the position of the neuron BDU, which undergoes a short anterior migration (J. Sulston, personal communication), was posterior to wild type 45% of the time (*n*=49).

migrating Q descendants correctly along the A/P axis (Fig. 9A).

Activation of the Hox gene *mab-5* within the migrating QL neuroblast

egl-20, *mig-14*, *mig-1* and *lin-17* act in the same pathway as the Hox gene *mab-5* to direct descendants of QL to migrate towards the posterior. All four of these genes act upstream of *mab-5*, and mutations in these genes appear to affect *mab-5* expression primarily in QL. None of these mutations appear to affect *mab-5* expression or activity globally; thus they are not likely to be general activators of *mab-5* unless their functions in other cells are redundant with other factors. These genes could act either at the level of transcription or of protein stability; however, the latter possibility seems less likely since mutations in these genes also block appearance of β-galactosidase in QL.a and QL.p in worms carrying *mab-5-lacZ* fusions encoding only the first seventeen amino acids of the MAB-5 protein (Salser and Kenyon, 1992; data not shown).

How might *egl-20*, *mig-14*, *mig-1* and *lin-17* function to activate *mab-5*? One possibility is that these genes are part of a system that creates left/right (L/R) asymmetries since, in wild type, QL but not QR expresses *mab-5*. Alternatively, these genes could be part of a system that is involved with the establishment of, or the response to, A/P positional information. In this model, the asymmetric initial migration would place QL and QR in different A/P positions, creating an A/P difference in addition to a L/R asymmetry. Signals present in QL's new posterior location would then instruct it to activate *mab-5*, allowing the A/P patterning system to distinguish the fate of QL from that of QR. Finally, it is possible that these genes act to specify aspects of Q cell fate in a manner independent of either A/P or L/R position.

One of these genes, *lin-17*, a homolog of the *Drosophila* tissue polarity gene, *frizzled* (Sawa et al., 1996), is required for many asymmetric cell divisions. For example, in *lin-17* mutants, many cells that normally divide to generate two different cell types (A and B) instead generate two similar cells (A and A) (Sternberg and Horvitz, 1988; Way et al., 1992). Although QL's ability to express *mab-5* is altered in *lin-17* mutants, it does not adopt the fate of its sister, the epidermal cell, V5. It is not clear how, or if, *lin-17*'s role in the generation and orientation of cellular asymmetry is related to its role in activating *mab-5* expression in QL. Molecular analysis of *lin-17*, as well as *egl-20*, *mig-14* and *mig-1*, should help to understand how *mab-5* gene expression is activated during the migration of QL.

The *egl-20* and *mig-14* genes influence the stopping points of the migrating Q descendants along the A/P axis

Two of the genes required for *mab-5* activation in QL, *egl-20* and *mig-14*, are also required in a *mab-5*-independent process to position cells correctly along the body axis. Mutations in these two genes cause the Q descendants to stop at positions that are further posterior than wild-type (Fig. 6). This shift is not due to misregulation of the Hox genes *mab-5*, *lin-39* or *egl-*

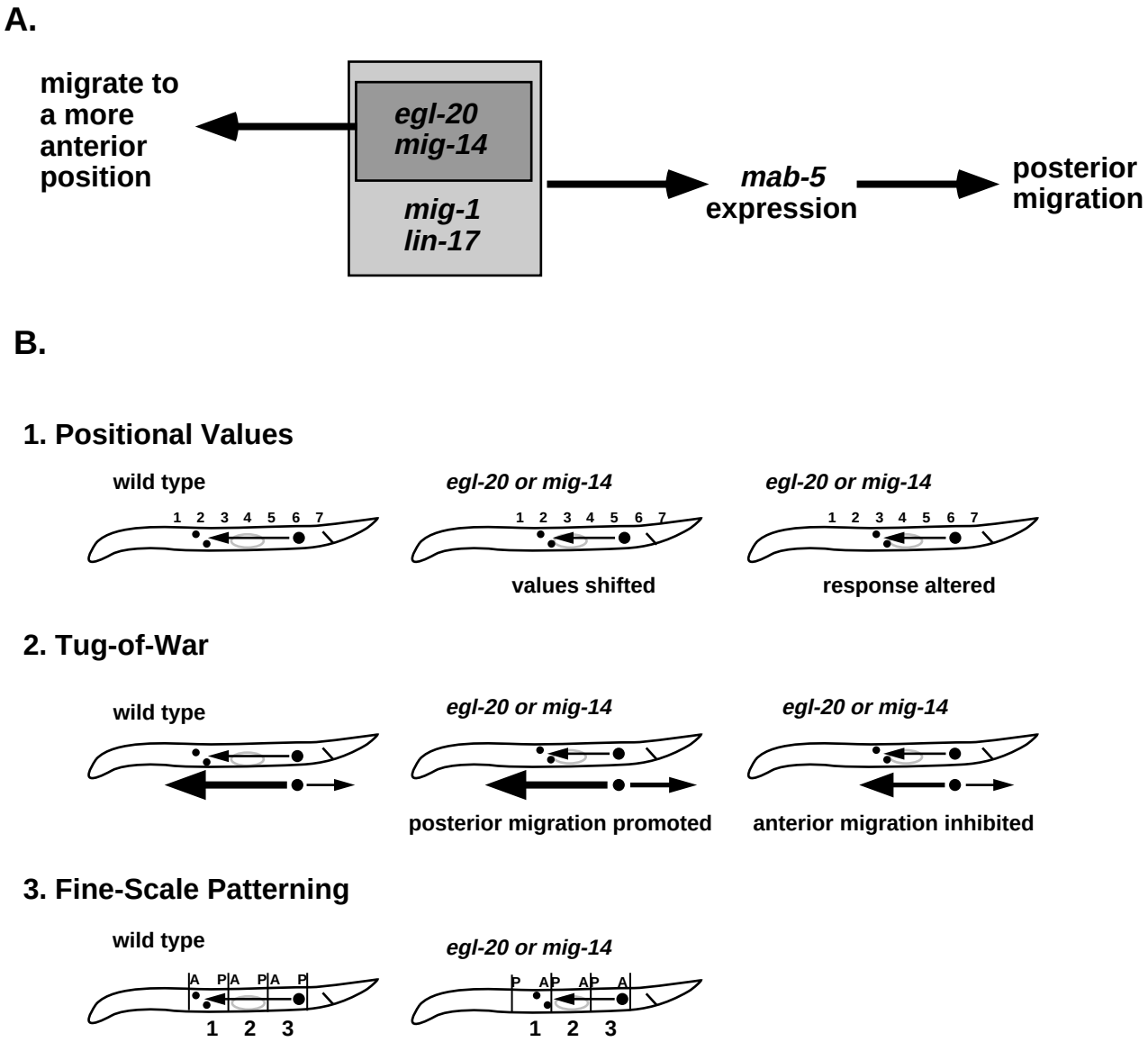

Fig. 9. (A) A diagram summarizing the roles of *egl-20, mig-14, mig-1* and *lin-17* in the migrations of the QL and QR descendants. These four genes activate *mab-5* expression in QL and its descendants, not QR and its descendants. Both *egl-20* and *mig-14*, however, promote anterior migration of the descendants of both QL and QR. (B) Alternative models to explain the posterior shift in *egl-20* and *mig-14* mutants. Large circle indicates the birthplace of QR. Arrows indicate the sum of the QR and QR.(d) migrations. Small circles indicate the positions of the QR.pa daughters. The position of the gonad primordium, represented by the gray oval, is not shifted in *egl-20* and *mig-14* mutants and is used as a reference point for Q.(d) cell position in these diagrams. **(1) Positional model.** The QR.(d) cells seek out specific positional values. *egl-20* and *mig-14* mutations either shift positional values toward the posterior (values shifted) or direct cells to migrate to more posterior positional values (response altered). In the former case, the cells continue to migrate to their wild-type positional value, but that value is now in a more posterior position in the worm. **(2) Tug-of-war model.** Proteins involved in anterior- and posterior-directed migrations compete for control of the QR.(d) cells. *egl-20* and *mig-14* mutations act by increasing the relative activity levels of proteins that promote posterior-directed migrations. **(3) Fine-scale patterning model.** QR.(d) cells migrate to the correct region of the body, then *egl-20* and *mig-14* help to position these cells correctly within that region. Mutations in *egl-20* and *mig-14* might disrupt fine-scale patterning, for example, by locally reversing A/P polarity.

5. Nor is the posterior shift due to a defect in motility, since mutations in *egl-20* and *mig-14* lengthen the posterior-directed migration of QR.ap in *mab-5(gf)* mutants, cause the non-migratory QR.p cell to migrate posteriorly in *mab-5(gf)* mutants, and reverse the direction of the anteriorly migrating QR.p cell in *mig-13* mutants (Fig. 7). The *egl-20* and *mig-14* mutations that we have analyzed all appear to reduce or eliminate gene function. Thus, it appears that the wild-type function of *egl-20* and *mig-14* is to allow the QR.(d) cells to migrate to more anterior positions.

Thus, in addition to directing both the QL and the QR descendants to more anterior positions, *egl-20(+)* and *mig-14(+)* also activate expression of *mab-5* in QL, which, in turn, promotes posterior migration. Since *mab-5* is not active in QR and its descendants, only the additional anterior increment is visible in the QR.(d) cell migrations, which migrate farther

towards the head. In the QL lineage, however, *egl-20(+)* and *mig-14(+)* promote both anterior migration (in a *mab-5*-independent way) and posterior migration (via *mab-5* regulation). Thus, in *egl-20* mutants, in which the *mab-5*-activation defect caused by *egl-20* is specifically suppressed by a *mab-5(gf)* mutation, the QL.(d) cells migrate too far posteriorly (Fig. 5), just as the QR.(d) cells do in this same double mutant (Fig. 6). This observation suggests that in the wild type, the anterior-directing and *mab-5*-activation (posterior-directing) functions of *egl-20* (and *mig-14)* combine to direct QL.p to stop and QL.a to migrate to its normal posterior position.

In migrations directed by signals from target cells, the attraction of migrating cells or growth cones to a specific target determines both their direction of migration and their stopping or turning point. In contrast, the Q.(d) cells do not migrate towards any apparent target, and yet they stop at precise positions. This situation is reminiscent of the targeting of chick retinal axons to specific positions in the optic tectum. Axons from cells in different regions of the retina map to specific locations on a tectum that morphologically appears relatively uniform. Graded expression of cell-surface molecules across the tectum may direct the migrating growth cones to different locations (reviewed by Tessier-Lavigne, 1995). If a similar graded signal guides the Q descendants, then *egl-20* and *mig-14*'s role must be relatively specific for Q.(d) cell migration, since many other A/P migrations are unaffected by mutations in these genes (Fig. 8).

Positioning migrating Q descendants along the A/P axis

How might *egl-20* and *mig-14* act to tell the migrating Q.(d) cells where to stop? There are at least three possibilities. (1) The Q.(d) cells might seek out specific positional values, perhaps defined by a specific concentration or combination of guidance molecules whose composition changes with position along the A/P axis. Mutations in *egl-20* and *mig-14* could act by shifting positional values, or the cell's perception of these values, towards the posterior (Fig. 9B). This model could also explain the failure of QL to activate *mab-5* if the decision to activate *mab-5* is based on a positional cue that is shifted out of the range of QL in *egl-20* or *mig-14* mutants. (2) Opposing forces within the Q.(d) cells could simultaneously promote both anterior- and posterior-directed migration. During this 'tug-of-war', the relative strength of the two opposing forces determines the final position of the migrating cell along the A/P axis (Fig. 9B). In this model, the wild-type function of *egl-20* and *mig-14* would be to promote anterior migration or inhibit posterior migration. (3) Mutations in *egl-20* and *mig-14* might disrupt fine-scale A/P patterning, in the manner of *Drosophila* segment polarity mutants (Howard, 1990; Ingham, 1991). *C. elegans* is not a segmented animal, but there are repeating patterns of cells along the body (for a discussion, see Kenyon and Wang, 1991). In this model, other gene products would guide Q.(d) cells to the correct region of the body, and then *egl-20* and *mig-14* would position them correctly within each metameric unit (Fig. 9B). Interestingly, mutations in *egl-20* can reverse the A/P polarity of certain epidermal cells (Jeanne Harris, Jennifer Whangbo and Cynthia Kenyon, unpublished data) and cells in the Q lineage (Fig. 3, legend), much as mutations in segment polarity genes do in the fly (Ma and Moses, 1995; Wehrli and Tomlinson, 1995).

Why do *egl-20* and *mig-14* mutations cause posterior shifts in the positions of cells in the Q lineage but not in the positions of all cells that migrate along the A/P axis? Migrations along the D/V axis are coordinately affected by *unc-5* and *unc-6* mutations, and migrations along the A/P axis, including the Q.(d) cells, are coordinately affected by mutations in *vab-8*. If common external cues guide all A/P cell migrations, then *egl-20* and *mig-14* might act to modify the response of the Q descendants to these signals. However, it remains possible that separate cell-extrinsic signals guide a subset of A/P cell migrations, such as those of the QL and QR descendants.

A new look at *mab-5*'s role in cell migration

Our analysis of the *egl-20* and *mig-14* mutant phenotypes suggests a new interpretation of *mab-5*'s role in cell migration. The starting point for the experiments presented here was the hypothesis that *mab-5* acts as a directional migration switch: if *mab-5* is on, the Q.(d) cells migrate towards the posterior, if *mab-5* is off, the Q.(d) cells migrate towards the anterior. In this model, it was assumed that *mab-5* acts to specify the direction of migration. Thus it was somewhat surprising to find that *mab-5* is not absolutely required to migrate posteriorly (in *mig-13; egl-20* double mutants; Fig. 7b).

This analysis of *egl-20* and *mig-14* mutations suggests the possibility that cells in the Q lineages are instructed to migrate to specific positions rather than in specific directions. In *egl-20* and *mig-14* mutants the target positions adopted by migratory cells are shifted posteriorly. In some cases, this positional shift involves a change in the direction of cell migration from anterior to posterior (Fig. 7). Perhaps this type of guidance system, that is, specifying cell position rather than direction of migration, governs Q.(d) cell migration. If so, then other mutations that alter the migrations of the Q.(d) cells would also act by respecifying target position rather than altering the direction of migration. Perhaps *mab-5*, rather than directing cells to migrate in a specific direction (i.e. towards the posterior), acts by directing cells to migrate to specific positions: positions that just happen to be posterior to the cells' starting points. The observation that intermediate levels of *mab-5* (as in a *mab-5/+* heterozygote) direct cells to intermediate positions (Salser and Kenyon, unpublished data), also suggests that *mab-5* may not act as a simple ON/OFF-type directional switch. Our results suggest that there are at least two ways to promote posterior migration of the Q descendants: through *mab-5* activity or by inhibiting the promotion of anterior migration by the *egl-20*/*mig-14* system, which can act independently of *mab-5*. Further analysis of *egl-20*, *mig-14*, *mig-1* and *lin-17*, both genetic and molecular, should provide a greater understanding of how guidance information is encoded in this system.

We thank members of our lab for discussions and comments on the manuscript and Raffi Aroian and Marc Tessier-Lavigne for comments on the manuscript. We are grateful to the anonymous reviewers for many helpful suggestions. We would also like to thank K. Nishiwaki for *mig-14(k124)*, M. Chalfie for the *mec-7-lacZ* transgenic worms, G. Xie and E. Aamodt for the *pag-1* mutant and advice on the *mec-7-lacZ* screen and G. Garriga for several *mig-1* mutants and the outcrossed *egl-20(n1437)* strain. We note that E. Hedgecock first observed that *mab-5(gf)* mutations suppress *mig-1*. We are grateful to Drs S. and K. Kocherlakota for advice on statistical analysis. Thanks to Judy Silber and Julin Maloof in the the Kenyon lab for the *egl-20* alleles *mu25* and *mu39*, to rotation students Monica Gerber and Martha Stark for constructing two double mutant strains and assisting in their analysis and

to Steve Salser for much patient assistance and advice on the β-galactosidase- and antibody-staining protocols. Some *C. elegans* strains were provided by the *Caenorhabditis* Genetics Center, which is funded by the NIH National Center for Research Resources (NCRR). This work was supported by NIH grant GM37053 and a grant from the Packard Foundation to C. K., an NSF predoctoral fellowship to N. T. R. and a UC Regents Fellowship to L. H.

REFERENCES

Ahn, J. and Fire, A. (1994). A screen for genetic loci required for body-wall muscle development during embryogenesis in *Caenorhabditis elegans*. *Genetics* **137,** 483-498.

Brenner, S. (1974). The genetics of *C. elegans*. *Genetics* **77,** 71-94.

Chalfie, M. and Sulston, J. (1981). Developmental genetics of the mechanosensory neurons of *C. elegans*. *Dev. Biol.* **82,** 358-370.

Chisholm, A. (1991). Control of cell fate in the tail region of *C. elegans* by the gene *egl-5*. *Development* **111,** 921-932.

Clark, S. G., Chisholm, A. D. and Horvitz, H. R. (1993). Control of cell fates in the central body region of *C. elegans* by the homeobox gene *lin-39*. *Cell* **74,** 43-55.

Costa, M., Weir, M., Coulson, A., Sulston, J. and Kenyon, C. (1988). Posterior pattern formation in *C. elegans* involves position-specific expression of a gene containing a homeobox. *Cell* **55,** 747-756.

Desai, C., Garriga, G., McIntire, S. L. and Horvitz, H. R. (1988). A genetic pathway for the development of the *Caenorhabditis elegans* HSN motor neurons. *Nature* **336,** 638-646.

Devore, D. L., Horvitz, H. R. and Stern, M. J. (1995). An FGF receptor signaling pathway is required for the normal cell migrations of the sex myoblasts in *C. elegans* hermaphrodites. *Cell* **83,** 611-620.

Ferguson, E. and Horvitz, H. (1985). Identification and characterization of 22 genes that affect the vulval cell lineages of the nematode *C. elegans*. *Genetics* **110,** 17-72.

Garriga, G., Desai, C. and Horvitz, H. R. (1993). Cell interactions control the direction of outgrowth, branching and fasciculation of the HSN axons of *Caenorhabditis elegans*. *Development* **117,** 1071-1087.

Godin, I., Wylie, C. and Heasman, J. (1990). Genital ridges exert long-range effects on mouse primordial germ cell numbers and direction of migration in culture. *Development* **108,** 357-363.

Hamelin, M., Scott, I. M., Way, J. C. and Culotti, J. G. (1992). The *mec-7* beta-tubulin gene of *Caenorhabditis elegans* is expressed primarily in the touch receptor neurons. *EMBO J.* **11,** 2885-2893.

Hedgecock, E. M., Culotti, J. G. and Hall, D. H. (1990). The *unc-5*, *unc-6* and *unc-40* genes guide circumferential migrations of pioneer axons and mesodermal cells on the epidermis in *C. elegans*. *Neuron* **4,** 61-85.

Hedgecock, E. M., Culotti, J. G., Hall, D. H. and Stern, B. D. (1987). Genetics of cell and axon migrations in *Caenorhabditis elegans*. *Development* **100,** 365-382.

Hodgkin, J., Edgley, M., Riddle, D. L. and Albertson, D. G. (1988). Appendix 4, Genetics. In *The Nematode Caenorhabditis elegans*, (ed. W. B. Wood), Cold Spring Harbor, New York: Cold Spring Harbor Laboratory.

Howard, K. (1990). The blastoderm prepattern. *Semin. Cell Biol.* **1,** 161-172.

Ingham, P. (1991). Segment polarity genes and cell patterning within the *Drosophila* body segment. *Current Opin. Genet. Dev.* **1,** 261-267.

Ishii, N., Wadsworth, W. G., Stern, B. D., Culotti, J. G. and Hedgecock, E. (1992). UNC-6, a laminin-related protein, guides cell and pioneer axon migrations in *C. elegans*. *Neuron* **9,** 873-881.

Jacobson, L. A., Jen, J. L., Hawdon, J. M., Owens, G. P., Bolanowski, M. A., Emmons, S. W., Shah, M. V., Pollock, R. A. and Conklin, D. S. (1988). Identification of a putative structural gene for cathepsin D in *Caenorhabditis elegans*. *Genetics* **119,** 355-363.

Kennedy, T. E., Serafini, T., de la Torre, J. R. and Tessier-Lavigne, M. (1994). Netrins are diffusible chemotropic factors for commissural axons in the embryonic spinal cord. *Cell* **78,** 425-435.

Kenyon, C. (1986). A gene involved in the development of the posterior body region of *C. elegans*. *Cell* **46,** 477-487.

Kenyon, C. and Wang, B. (1991). A cluster of Antennapedia-class homeobox genes in a nonsegmented animal. *Science* **253**, 516-517.

Ma, C. and Moses, K. (1995). *wingless* and *patched* are negative regulators of the morphogenetic furrow and can affect tissue polarity in the developing *Drosophila* compound eye. *Development* **121,** 2279-2289.

Montell, D. J. (1994). Moving right along: regulation of cell migration during *Drosophila* development. *Trends Genet.* **10,** 59-62.

Robinson, N. T. (1995). Genetic Analysis of Neuroblast Migration in *Caenorhabditis elegans*. Ph.D. thesis, University of California, San Francisco.

Salser, S. and Kenyon, C. (1992). Activation of a *C. elegans Antennapedia* homolog within migrating cells controls their direction of migration. *Nature* **355,** 255-258.

Salser, S., Loer, C. and Kenyon, C. (1993). Multiple HOM-C gene interactions specify cell fates in the nematode central nervous system. *Genes Dev.* **7,** 1714-1724.

Salser, S. J. and Kenyon, C. (1996). A *C. elegans* Hox gene switches ON, OFF, ON, and OFF again to regulate proliferation, differentiation, and morphogenesis. *Development* **122,** 1651-1661.

Sawa, H., Lobel, L. and Horvitz, H. R. (1996). The *Caenorhabditis elegans* gene *lin-17*, which is required for certain asymmetric cell divisions, encodes a putative seven-transmembrane protein similar to the *Drosophila* Frizzled protein. *Genes Dev.* (in press).

Serafini, T., Kennedy, T. E., Galko, M. J., Mirzayan, C., Jessel, T. M. and Tessier-Lavigne, M. (1994). The netrins define a family of axon outgrowth promoting proteins homologous to *C. elegans* UNC-6. *Cell* **78,** 409-424.

Shaller, D., Wittmann, C., Spicher, A., Muller, F. and Tobler, H. (1990). Cloning and analysis of three new homeobox genes from the nematode *Caenorhabditis elegans*. *Nucl. Acids Res.* **18,** 2033-2036.

Sternberg, P. W. and Horvitz, H. R. (1988). *lin-17* mutations of *Caenorhabditis elegans* disrupt certain asymmetric cell divisions. *Dev. Biol.* **130,** 67-73.

Stringham, E. G. and Candido, E. P. (1993). Targeted single-cell induction of gene products in *Caenorhabditis elegans*: a new tool for developmental studies. *J. Exp. Zool.* **266,** 227-233.

Sulston, J. and Hodgkin, J. (1988). Methods. In *The Nematode Caenorhabditis elegans* (ed. W. B. Wood), pp. 587-605. Cold Spring Harbor, New York: Cold Spring Harbor Laboratory Press.

Sulston, J. and Horvitz, H. R. (1977). Post-embryonic cell lineages of the nematode, *C elegans*. *Dev. Biol.* **56,** 110-156.

Teragawa, C. and Bode, H. (1990). Spatial and temporal patterns of interstitial cell migration in Hydra vulgaris. *Dev. Biol.* **138,** 63-81.

Tessier-Lavigne, M. (1995). Eph receptor tyrosine kinases, axon repulsion, and the development of topographic maps. *Cell* **82**, 345-348.

Trent, C., Tsung, N. and Horvitz, H. R. (1983). Egg-laying defective mutants of the nematode *C. elegans*. *Genetics* **104,** 619-647.

Wang, B. B., Müller-Immergluck, M. M., Austin, J., Robinson, N. T., Chisholm, A. and Kenyon, C. (1993). A homeotic gene cluster patterns the anteroposterior body axis of *C. elegans*. *Cell* **74,** 29-42.

Way, J., Run, J. and Wang, A. (1992). Regulation of anterior cell-specific *mec-3* expression during asymmetric cell division in *C. elegans*. *Dev. Dynam.* **194,** 289-302.

Wehrli, M. and Tomlinson, A. (1995). Epithelial planar polarity in the developing *Drosophila* eye. *Development* **121,** 2451-2459.

White, J., Southgate, E., Thomson, J. and Brenner, S. (1986). The structure of the nervous system of the nematode *C. elegans*. *Philosophical Transactions of the Royal Society of London* **314B,** 1-340.

Wightman, B., Clark, S. G., Taskar, A. M., Forrester, W. C., Maricq, A. V., Bargmann, C. I. and Garriga, G. (1996). The *C. elegans* gene *vab-8* guides posteriorly directed axon outgrowth and cell migration. *Development* **122,** 671-682.

Williams, B. D., Schrank, B., Huynh, C., Shownkeen, R. and Waterston, R. H. (1992). A genetic mapping system in *Caenorhabditis elegans* based on polymorphic sequence-tagged sites. *Genetics* **131,** 609-624.

Xie, G. Y., Jia, Y. and Aamodt, E. (1995). A *C. elegans* mutant screen based on antibody or histochemical staining. *Genetic Analysis: Biomolecular Engineering* **12,** 95-100.

(Accepted 17 July 1996)